Swarm-derived indices of geomagnetic activity

Constantinos Papadimitriou[1,2,3], Georgios Balasis[1], Adamantia Zoe Boutsi[1,2], Alexandra Antonopoulou[1], Georgia Moutsiana[2], Ioannis A. Daglis[2,4,1], Omiros Giannakis[1], Paola de Michelis[5], Giuseppe Consolini[6], Jesper Gjerloev[7], Lorenzo Trenchi[8]

[1]IAASARSNational Observatory of Athens, Athens, Greece
[2]Department of Physics, National & Kapodistrian University of Athens, Athens, Greece
[3]Space Applications & Research Consultancy, SPARC G.P., Athens, Greece
[4]Hellenic Space Center, Athens, Greece
[5]Istituto Nazionale di Geofisica e Vulcanologia, Rome, Italy
[6]INAFIstituto di Astrofisica e Planetologia Spaziali, Rome, Italy
[7]Johns Hopkins University Applied Physics Laboratory, USA
[8]ESRIN, European Space Agency, Italy

Key Points:

- New geomagnetic activity indices based on Swarm magnetic field data are computed similar to standard ground-based indices of Dst, ap and AE
- Swarm-derived indices show excellent correlations with both the traditional and SuperMAG-derived indices
- Swarm-based AE index enable us to monitor substorm activity also at the southern hemisphere

Corresponding author: Constantinos Papadimitriou, `constantinos@noa.gr`

Abstract

Ground-based indices, such as the Dst, ap and AE, have been used for decades to describe the interplay of the terrestrial magnetosphere with the solar wind and provide quantifiable indications of the state of geomagnetic activity in general. These indices have been traditionally derived from ground-based observations from magnetometer stations all around the Earth. In the last 7 years though, the highly successful satellite mission Swarm has provided the scientific community with an abundance of high quality magnetic measurements at Low Earth Orbit (LEO), which can be used to produce the space-based counterparts of these indices, such the Swarm-Dst, Swarm-ap and Swarm-AE indices. In this work, we present the first results from this endeavour, with comparisons against traditionally used parameters. We postulate on the possible usefulness of these Swarm-based products for a more accurate monitoring of the dynamics of the magnetosphere and thus, for providing a better diagnosis of space weather conditions.

Plain Language Summary

Ground-based geomagnetic activity indices, like Dst, ap and AE, have been used for decades to monitor the dynamics of the Earth's magnetosphere, and provide information on two major types of space weather phenomena, i.e., magnetic storm and magnetospheric substorm occurrence and intensity. This study demonstrates how magnetic field data from a Low Earth Orbit (LEO) satellite mission, like ESA's Swarm constellation, can be used to derive corresponding space-based geomagnetic activity indices. The comparison of Swarm-based with ground-based indices shows a very good agreement, indicating that Swarm magnetic field data can be used to provide new satellite-based global indices to monitor the level of geomagnetic activity. Given the fact that the official AE is constructed by data from 12 ground stations solely in the northern hemisphere and the official ap from only 2 stations in the southern hemisphere (and 11 in the northern one), it can be said that both of these indices are predominantly northern, while the Swarm-derived AE and ap indices may be more representative of a global state, since they are based on measurements from both hemispheres.

1 Introduction

The magnetosphere is a highly complex system of fields and currents that envelop the Earth and interact with each other producing a wide range of phenomena. One particular current system that holds special importance is the aptly named ring current. The ring current is a toroidal electric current flowing around the Earth, formed by the azimuthal motion of electrons and ions, extending from 3 to 8 Earth radii on the mangetospheric equatorial plane (Daglis et al., 1999). Because of its shape and direction, it forms its own magnetic field component, with an axis almost parallel to that of the Earths dipole and the same polarity (southward). A direct consequence of this is that on the surface of our planet the ring currents induced magnetic field is opposite to the Earth's magnetic field. Thus, in cases where incoming current systems of the solar wind have the appropriate properties to cause particle injection in the inner magnetosphere and enhance the ring current, the terrestrial field on the surface of the planet will exhibit a decrease due to the increase of the counteracting ring current field. This is the phenomenon known as geomagnetic (or simply magnetic) storm, which seriously affects the electromagnetic environment of the Earth and can cause a wide range of significant effects ranging from telecommunication issues and satellite failures to the induction of high voltage electrical currents on electrical wires and conducting materials on the surface of the planet (Bothmer and Daglis, 2007). The monitoring of geomagnetic storms has been traditionally accomplished by means of the Disturbance storm-time (Dst) index, which represents the axially symmetric disturbance of the horizontal component of the magnetic field at the magnetic equator on the Earth's surface (Sugiura and Kamei, 1981). As such, it oper-

ates as a proxy for the enhancement and subsequent weakening of the ring current and hence the onset and evolution of magnetic storms.

Another group of current systems that cause an array of spectacular phenomena are the auroral electrojets, which are currents that flow in concentrated channels of high conductivity in the Earths ionosphere and are carried by particles that generate the auroral light, moving both eastward (therefore forming the East ElectroJet EEJ) and westward (therefore forming the West ElectroJet WEJ). Related to these systems are the disturbances known as magnetospheric substorms (Akasofu, 1964; McPherrron, 1979), which are collective phenomena, considered as one of the major ways for the discharge of accumulated energy in the terrestrial magnetosphere (Chian and Kamide, 2007). During the onset of substorm expansion phase, a dynamical process in the near Earth magnetosphere causes cross tail current to be diverted into the ionosphere, forming a substorm current wedge consisting of downward (upward) field aligned currents on the dawnside (duskside) of the wedge and a westward auroral electrojet in the ionosphere (Kepko at al., 2015). The Auroral Electrojet index AE (Davis and Sugiura, 1966) actually measures the intensity of this substorm enhanced westward ionospheric electrojet via its diamagnetic result on the horizontal component of the terrestrial magnetic field.

Balasis et al. (2019) recently derived a 1 Hz Swarm Dst-like index based solely on magnetic data from the Swarm mission. The scientific merit of such a geomagnetic activity index relies on its global character (since the three satellites provide a global Earth coverage both latitudinally and longitudinally), as well as their proximity to the region of emergence and activity of ionospheric currents. The present work further expands upon that first effort, by simplifying and at the same time generalizing the approach so that all three most commonly used indices of geomagnetic activity can be derived, namely Dst, ap (or Kp) and AE. This article is divided upon 6 sections. Following the Introduction, Section 2 presents the main steps of analysis and pre-processing of Swarm data that must be taken before the method is applied, as well as the argumentation on the selection of an appropriate time interval for the demonstration of the effectiveness of the methods. Section 3 outlines the new process for the derivation of the Swarm-Dst index and is complemented by a comparison against the standard Dst index. The same line of thinking is followed in Sections 4 and 5, correspondingly for the ap and AE indices, while Section 6 summarizes the findings and offers some general remarks on the usefulness of the method.

2 Data Selection and Pre-processing

Our explorers in this quest for an ever more detailed description of the Earth's magnetic field are the satellites of the Swarm constellation (Friis-Christensen et al., 2006). Launched on 23 November 2013, the mission is composed of three satellites in polar Low-Earth Orbit (LEO), with two of them (Swarm-A and Swarm-C) flying side by side at an initial altitude of 460 km and the third (Swarm-B) flying slightly higher at 510 km. Carrying highly precise instruments, the mission offers the most up-to-date survey of the terrestrial magnetic field (De Michelis et al., 2015; Hulot et al., 2015; Olsen et al., 2015), but also of the general near-Earth electromagnetic environment and its interaction with the solar wind (Balasis et al., 2015; Olsen et al., 2016; Papadimitriou et al., 2018).

The derivation of the Swarm indices is based on the dataset prepared within the framework of the INTENS (Characterization of IoNospheric TurbulENce level by Swarm constellation) project. The dataset was constructed from the Level 1b, MAG_LR product of the Swarm mission (https://swarm-diss.eo.esa.int/), which contains among others, magnetic field measurements from the Vector Field Magnetometer (VFM) instrument (Tffner-Clausen et al., 2016) on board the three satellites at a time sampling of 1 second. The magnetic field vector was mapped to Mean Field Aligned (MFA) coordinates, i.e. one component parallel to the mean field B_{par} and two perpendicular com-

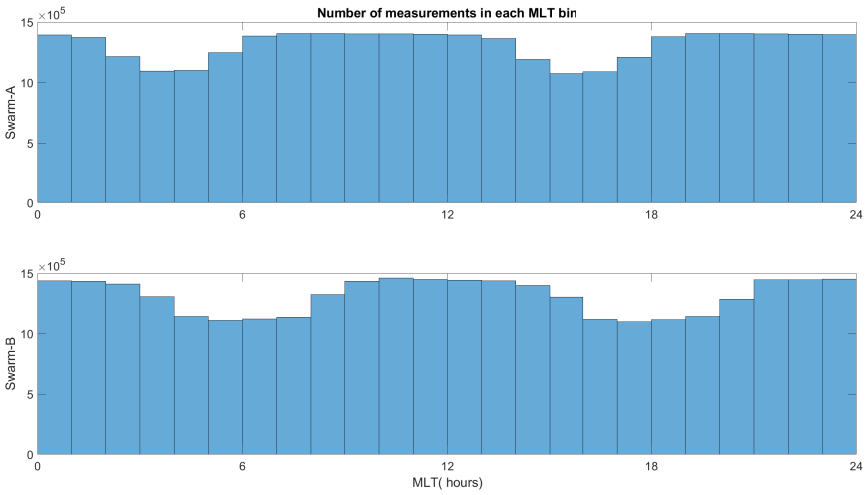

Figure 1. Number of measurements performed by the Swarm satellites in each MLT bin. Top panel shows Swarm-A (Swarm-C is identical) and bottom panel Swarm-B.

ponents B_{per1} and B_{per2} and the static, background field was subtracted by removing the internal mode of the CHAOS-6 model (Finlay et al., 2016) from the data, which consists of the core and crustal magnetic field contributions of the Earth. Obvious outliers, i.e. isolated spikes, were removed by applying a simple threshold and as a final step, the magnitude of the residual vector was computed and saved for further processing.

The time period that we selected for the illustration of the method was the year of 2015, which is appropriate to test the Swarm indices during both quiet and disturbed geomagnetic conditions. Indeed, 2015 was characterized by two months of intense geomagnetic activity due to the storms of March 17$^{\text{th}}$ and June 23$^{\text{rd}}$, two events that have been extensively discussed by the scientific community (Liu et al., 2015; Kataoka et al., 2015; Wang et al., 2016; Wu et al., 2016; Marubashi et al., 2016; Balasis et al., 2018; De Michelis et al., 2020), as well as a third event of less intensity, yet still an important one, the storm of the 22$^{\text{nd}}$ of December. Additionally, several substorms erupted between and following the storm events, which had shorter duration and thus were interspersed by several quiet intervals as well. As such, this period provides a blend of both storm and substorm activity, while also exhibiting intervals of quiescence and is perfectly suited for modelling all levels of geomagnetic activity.

A duration that is a multiple of a four-month interval is also important for reasons of geographical coverage, as four months is the time it takes for the orbital plane of the Swarm satellites to complete a 180° turn, with respect to the Sun-Earth line. Since the satellites fly one half of their orbit on the day-side and the other half on the night-side, a 180° rotation provides full local time (LT) coverage. The time spent by the Swarm satellites in each bin of Magnetic Local Time (MLT) is shown in Figure 1 (only one of the satellites of the lower pair is shown, Swarm-A and not Swarm-C, since their orbits are almost identical).

3 The Swarm-derived Dst Index

Magnetic storms produce global magnetic disturbances on the Earth's surface, which serve as the basis for storm monitoring via the hourly Dst index. It is derived from the variations of the horizontal component of the terrestrial magnetic field, using data from

four observatories, positioned at magnetic latitudes ranging from approximately -30° to +30°.

In order to mirror the behaviour of the ground station data, it is imperative to remove measurements that were performed when the satellites were at high latitudes. Thus, the first step in the process is to discard times where the satellites were above +30° or below -30° in magnetic latitude. At those near-equatorial latitudes, a good proxy for the horizontal component of the terrestrial magnetic field is the B_{par}, so the process continues keeping only this component and ignoring the others. Then, a non-overlapping, moving average scheme is applied on the time series, with a window of 60 seconds, so that the series are now set to a 1-minute time resolution. Up to this point, the analysis was performed separately for each of the satellites Swarm-A and Swarm-B (Swarm-C yields the same results as A so it was not used). In the next step the two series are merged, in a joint 1-min resolution dataset, so that if both satellites are concurrently within the latitude limits their values are averaged, otherwise we keep only the ones from the satellite that was within the prescribed latitudes. Even so, there are still many cases for which all satellites are at high latitudes, so these gaps are interpolated by a simple linear scheme, to produce a complete time series. Then, a low-pass, Chebyshev Type I filter is used, with a cutoff period of 4 hours, to filter out some of the small perturbations in the signal that arise from the fast motion of the satellites. Finally, we apply a linear transform of the form:

$$\mathbf{S_{Dst} = 1.53 B_f + 12.85}$$

where B_f is the filtered series acquired in the last step, to get the final Swarm-Dst index S_{Dst}. A flowchart of the method, showing the form of the time series at each intermediate step described here is shown in Figure 2. A comparison of the final Swarm index with the traditionally used one is shown in Figure 3, where it is evident how this method can produce an index that is strikingly similar to the traditionally used one, a similarity that is justified by a Pearson correlation coefficient (Pearson, 1895) of 0.94 between the two. It should be noted here that to facilitate comparisons, the SYM-H index was used instead of the Dst, since it is provided with a 1-minute sampling time, instead of the hourly series of the official Dst index, but the good agreement holds also with the official Dst, since the two indices are practically identical (Iyemori et al., 2010).

The four parameters of the method are the latitudinal limit, the filtering cutoff and the two parameters of the linear transform. Even though their choice is intuitive in this case, a more formal derivation is achieved by following two simple steps. First, many different combinations for the latitudes and filtering cutoff are tested, trying to find the one that maximizes the correlation with the ground-based index series and secondly, keeping the first two constant, we find the linear transform parameters that minimize the root mean square error between the filtered series and the standard index.

4 The Swarm-derived ap Index

The geomagnetic three-hourly Kp index was introduced by J. Bartels in 1949 and is derived from 13 magnetic observatories, 11 of which in the Northern Hemisphere, between latitudes from +38° up to +60° and 2 in the Southern Hemisphere at latitudes of -43° and -35° [https://www.gfz-potsdam.de/en/kp-index/]. It is designed to measure solar particle radiation by its magnetic effects and today it is considered a proxy for the energy input from the solar wind to Earth. The name Kp was derived from the German words “planetarische Kennziffer meaning “planetary index. The index is quasi-logarithmic in nature and since this is more difficult to assign to actual magnetic field measurements, Bartels also proposed a correspondence between Kp values and the more linear ap index values. Due to this, we will also use the ap index for this study, keeping in mind that a simple one-to-one relation can map the ap values to Kp and vice-versa.

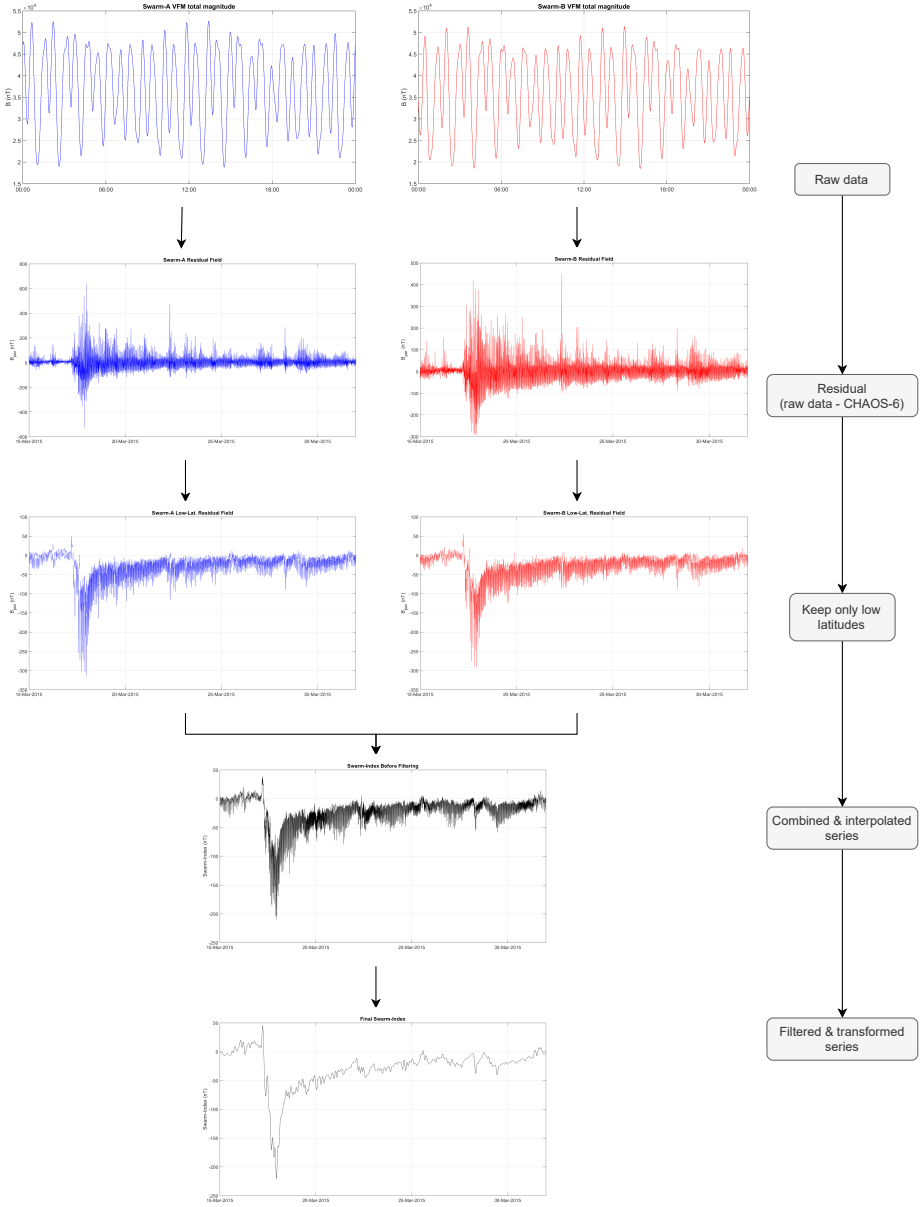

Figure 2. Flowchart for the derivation of the Swarm-Dst index. Each of the 3 upper rows includes distinct panels for Swarm-A (blue) and Swarm-B (red) time series, while each of the next 2 rows shows a single panel of combined Swarm-A and Swarm-B time series.

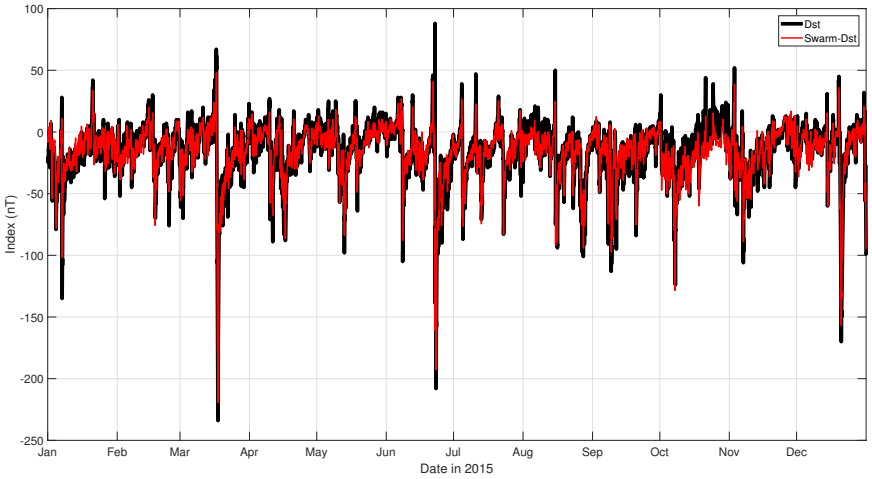

Figure 3. Swarm-derived Dst index (red) compared to the ground-based index (black).

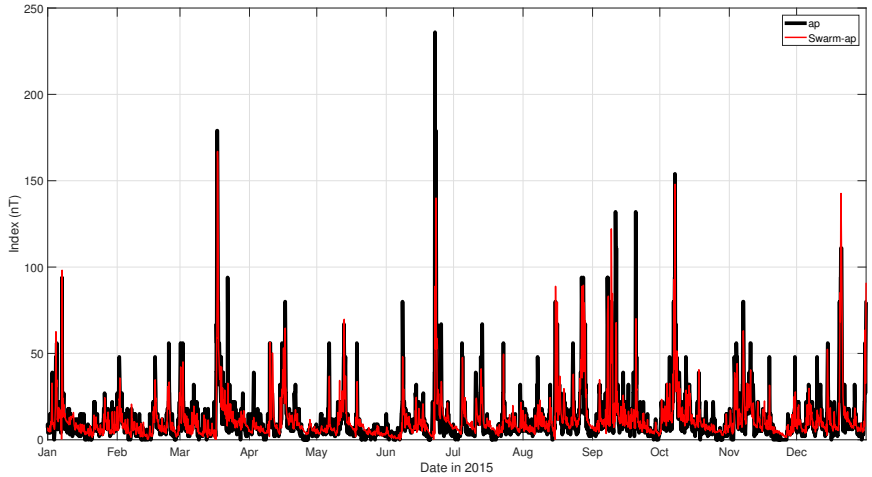

Figure 4. Swarm-derived ap index (red) compared to the standard index (black).

We repeat the exact same process as above, tweaking the parameters until the best possible outcome emerges. For the Swarm-ap index we use measurements of the magnitude of the residual field vector, located in a narrow band between +55° and +60° in the Northern Hemisphere and correspondingly -60° to -55° in the Southern one. The cut-off period is set to 9 hours and the linear transform to $S_{ap} = 0.39B_f - 4.29$ in order to achieve a maximum correlation coefficient of 0.86. The result is shown in Figure 4. As can be seen the Swarm index closely follows the standard ap index, missing only in absolute magnitude a few of the highest peaks. This hints at the possibility of a non-linear transform which would promote high values more significantly than the lower ones, something which makes sense given the peculiar way with which these indices are produced.

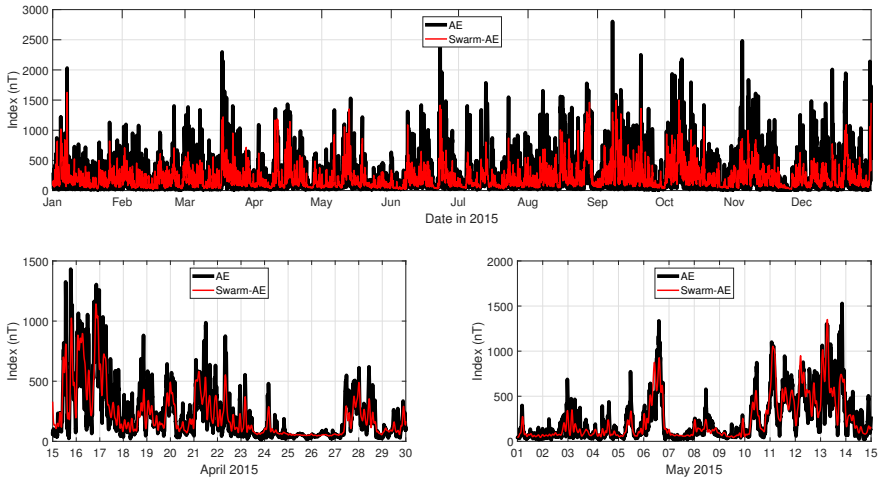

Figure 5. Swarm-derived AE index (red) compared to the standard AE index (black). Top panel shows the entire 12 month period from Jan 1st to Dec 31st 2015, while the two bottom panels show zoomed pictures from the second half of April (bottom left) and first half of May (bottom right).

5 The Swarm-derived AE Index

The AE index represents the overall activity of the electrojets. The AE index is derived from geomagnetic variations in the horizontal component observed at selected observatories along the auroral zone, solely in the Northern Hemisphere, at magnetic latitudes between +60° and +70° [http://wdc.kugi.kyoto-u.ac.jp/aedir/ae2/onAEindex.html]. To mirror this we follow the same process outlined above, again for the magnitude of the residual field, keeping only measurements between +65° and +75° (and correspondingly -75° to -65°) in magnetic latitude, filtering with a cutoff period of 2.6 hours and applying the transform $S_{AE} = 2.2B_f - 8.9$ to achieve a maximum correlation coefficient of 0.85. As can be seen in Figure 5, while the Swarm index doesn't match the peaks during the intense storm events (again hinting at a possible non-linear relation), it captures with high accuracy the substorm activity during April and May, highlighted with the two bottom panels which zoom in two characteristic intervals.

One of the most important benefits of using a satellite observatory is that by slightly changing the formulation of the method, one can easily produce more localized versions of these indices. As an example, by imposing the latitudinal limits to only maintain measurements from the north or the south hemisphere, while keeping the rest of the method unchanged, we can construct the Swarm-AE-North and Swarm-AE-South indices, to complement the full version of Swarm-AE. This is shown in Figure 6, where the full Swarm-AE index is overplotted by its localized North and South hemisphere counterparts. Even though the two localized indices agree, in general, with each other, if we draw our attention to specific, small intervals, like the ones depicted on the two bottom subplots of Figure 6, one can see small, but important differences between the two. This comes as a verification of recent literature (Liou et al., 2018) in which they report that substorm onset is far from north-south symmetric, as was previously considered, and that it is more likely to be initiated in a dark than a sunlit oval. They additionally showed that the preferred locations of substorm onsets coincide with the local peak of the Earths magnetic field (or a minimum in the ionospheric conductivity), a finding which is consistent with

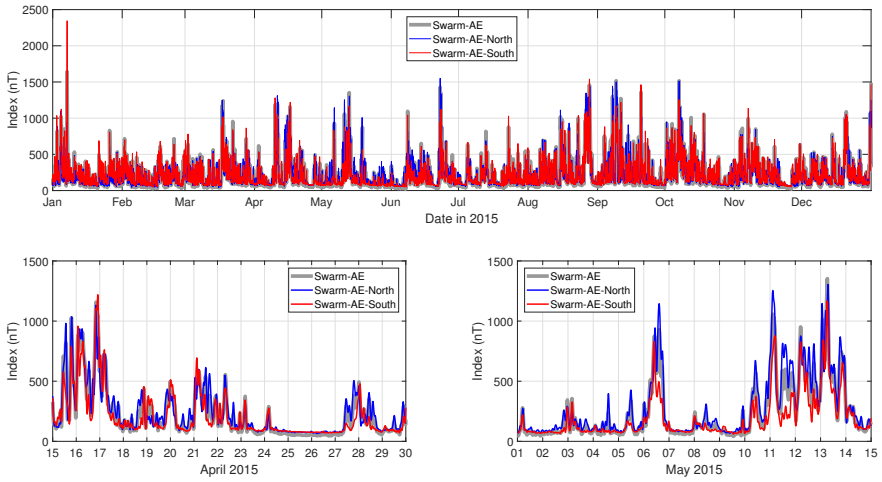

Figure 6. Swarm-derived AE index (grey) compared to its regional counterparts the Swarm-AE-North (blue) and Swarm-AE-South (red) indices. Top panel shows the entire 12 month period from Jan 1st to Dec 31st 2015, while the two bottom panels show zoomed pictures from the second half of April (bottom left) and first half of May (bottom right).

an ionospheric feedback mechanism. Similar asymmetries were also reported by Weygand et al. (2014) based on magnetic field data from ground based observatories.

6 Comparisons against SuperMAG Indices

There has been a huge effort in recent years to complement the traditional indices of geomagnetic activity with new versions, utilizing data from the immense ground magnetometer network SuperMAG. SuperMAG is a worldwide collaboration of organizations and national agencies which currently operate more than 300 ground-based magnetometers spread across the globe (Gjerloev, 2009). Data from each of these stations are processed according to the same guidelines (Gjerloev, 2012) and utilized, according to their latitudinal location to produce the SuperMAG geomagnetic activity indices: the SMR index, which is a ring current index, similar to Dst or SYM-H (Newell et al., 2012) and the SME index, which attempts to capture the auroral electrojet behavior and thus operate in a manner analogous to the AE index (Newell et al., 2011). As a first step to incorporate these new indices in our work, we performed two simple comparisons, calculating the correlation coefficient between the Swarm-Dst and the SuperMAG SMR index, which yielded a value of 0.95 and also compared Swarm-AE (the full version) against SuperMAG SME, which gave the result 0.86. Both of these values are slightly higher than the ones procured by comparisons against the traditional SYM-H and AE indices, which indicates that the satellite indices are closer to the new indices, which are more detailed and are being produced by many more observatories than the old ones, although further work is needed to address these differences properly. That being said, this is a very promising result that we believe further justifies our approach and opens new avenues for exploration.

These results, along with all the previous ones, are presented in Table 1, while a pictorial representation of this comparison is shown in Figure 7.

Table 1. Summary of results

Correlations with ring current indices	
Swarm-Dst vs SYM-H	0.94
Swarm-Dst vs SMR	0.95
Correlations with ap index	
Swarm-ap vs ap	0.86
Correlations with auroral electrojet indices	
Swarm-AE vs AE	0.85
Swarm-AE vs SME	0.86
Swarm-AE-North vs AE	0.81
Swarm-AE-South vs AE	0.77

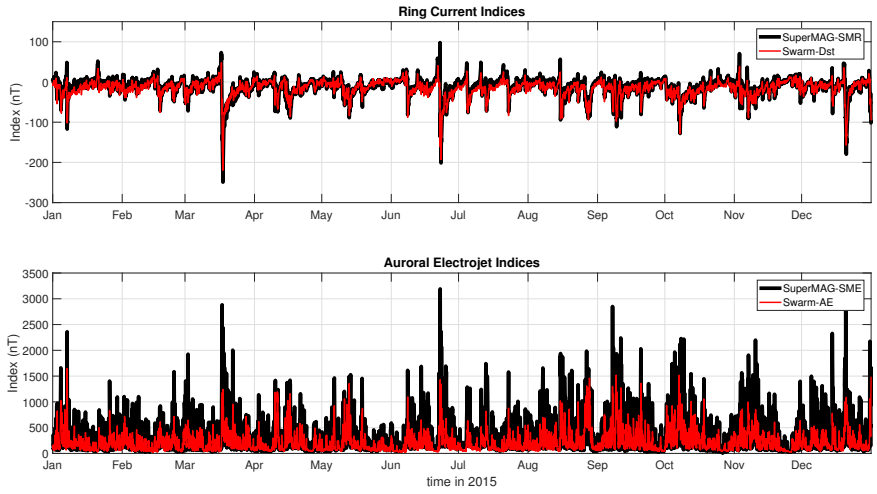

Figure 7. Comparions of SuperMAG indices (with black) SMR (top panel) and SME (bottom panel) against their Swarm-derived counterparts (with red) for the year 2015.

7 Discussion and Conclusions

This work shows how the magnetic field data from the Swarm mission can be utilized, by means of a simple and intuitive method to reproduce, with high accuracy, the three major indices of geomagnetic activity, namely the Dst, ap (or Kp) and AE indices. The global coverage provided by a constellation of low-Earth orbiting satellites makes them ideal for encapsulating the entirety of the magnetic field, discerning changes at larger spatial scales, while their altitude positions them right in the place of the ionospheric currents which are responsible for many of the effects that comprise our notion of space weather. We note that the Swarm AE-like index could, in principle, be more representative of a global state, since it is based on measurements from both hemispheres, while the ground-based one is computed from measurements in the Northern Hemisphere only.

Additionally, since the satellites remain at fairly constant LTs for several weeks, their data can further promote recent research on regional indices of electrojet or ring current activity, such as the regional versions of SME and SMR indices (Bergin et al., 2020). As such, satellite magnetic observatories can complement their ground-based counterparts, providing new insights into the state of the magnetosphere and new promise for more accurate diagnosis of space weather conditions.

Acknowledgments

The results presented rely on data collected by the three satellites of the Swarm constellation. We thank the European Space Agency (ESA) that supports the Swarm mission. Swarm data can be accessed at http://earth.esa.int/swarm. We acknowledge the Kyoto World Data Center (WDC) for Geomagnetism and the observatories that produce and make Dst, ap and AE indices available at http://wdc.kugi.kyoto-u.ac.jp/. We gratefully acknowledge the SuperMAG collaborators for the provision of ground-based index data (https://supermag.jhuapl.edu/info/?page=acknowledgement). The authors acknowledge financial support from European Space Agency (ESA contract N. 4000125663/18/I-NB "EO 486 Science for Society Permanently Open Call for Proposals EOEP-5 BLOCK4" (INTENS)). This work was benefited from discussions within the International Space Science Institute (ISSI) Team # 455 "Complex Systems Perspectives Pertaining to the Research of the Near-Earth Electromagnetic Environment".

References

Akasofu, S.-I. (1964). The development of the auroral substorms. *Planet. Space Sci.*, 12, 273.

Balasis, G., Papadimitriou, C., Daglis, I. A., and Pilipenko, V. (2015). ULF wave power features in the topside ionosphere revealed by Swarm observations. *Geophys. Res. Lett.*, 42, 6922-6930, doi:10.1002/2015GL065424.

Balasis, G., et al. (2018). Observation of intermittency-induced critical dynamics in geomagnetic field time series prior to the intense magnetic storms of March, June, and December 2015. *J. Geophys. Res.: Space Phys.*, 123, 4594-4613, doi:10.1002/2017JA025131.

Balasis, G., Papadimitriou, C., and Boutsi, A. Z. (2019). Ionospheric response to solar and interplanetary disturbances: a Swarm perspective. *Philosophical Transactions A*, doi:10.1098/rsta.2018.0098.

Bartels, J. (1949). The standardized index Ks and the planetary index Kp. *IATME Bull.* 12 (b), 97, IUGG Publ.

Bothmer, V., and Daglis, I. A. (2007). In V. Bothmer and I. A. Daglis (Eds.), *Space Weather: Physics and Effects*, Praxis/Springer, New York, (438 pp.), ISBN 978-3-540-23907-9.

Bergin, A., Chapman, S., and Gjerloev, J. (2020). AE, Dst and their SuperMAG Counterparts: The Effect of Improved Spatial Resolution in Geomagnetic

Indices. *J. Geophys. Res.: Space Physics*, 125, doi:10.1029/2020JA027828.

Chian, A. C.-L., and Kamide, Y. (2007). An Overview of the Solar-Terrestrial Environment. In Y. Kamide and A. C.-L. Chian (Eds.), *Handbook of the Solar-Terrestrial Environment*, Springer-Verlag, Berlin, Heidelberg, doi:10.1007/978-3-540-46315-3.

Daglis, I. A., Thorne, R. M., Baumjohann, W., and Orsini, S. (1999). The terrestrial ring current: Origin, formation, and decay. *Rev. Geophys.*, 37(4), 407-438, doi:10.1029/1999RG900009.

Davis, T. N., and Sugiura, M. (1966). Auroral electrojet activity index AE and its universal time variations. *J. Geophys. Res.*, 71(3), 785801, doi:10.1029/JZ071i003p00785.

De Michelis, P., Consolini, G., and Tozzi, R. (2015). Magnetic field fluctuation features at Swarms altitude: A fractal approach. *J. Geophys. Res.*, 42, 31003105, doi:10.1002/2015GL063603.

De Michelis, P., Pignalberi, A., Consolini, G., Coco, I., Tozzi, R., and Pezzopane, M., et al. (2020). On the 2015 St. Patrick's storm turbulent state of the ionosphere: Hints from the Swarm mission. Journal of Geophysical Research: *Space Physics*, 125, e2020JA027934. https://doi.org/10.1029/2020JA027934

Finlay, C., et al. (2016). Recent geomagnetic secular variation from Swarm and ground observatories as estimated in the CHAOS-6 geomagnetic field model. *Earth Planets and Space*, 68, 112, doi:10.1186/s40623-016-0486-1.

Friis-Christensen, E., Lhr, H., and Hulot, G. (2006). Swarm: A constellation to study the Earths magnetic field. *Earth Planets Space*, 58, 351358, doi:10.1186/BF03351933.

Gjerloev, J. W. (2009). A global ground-based magnetometer initiative. *Eos Trans. AGU*, 90 (27), 230231, doi:10.1029/2009EO270002.

Gjerloev, J. W. (2012). The SuperMAG data processing technique. *J. Geophys. Res.*, 117, A09213, doi:10.1029/2012JA017683.

Hulot, G., Vigneron, P., Lger, J.-M., Fratter, I., Olsen, N., Jager, T., Bertrand, F., Brocco, L., Sirol, O., Lalanne, X., Boness, A., and Cattin, V. (2015). Swarms absolute magnetometer experimental vector mode, an innovative capability for space magnetometry. *Geophys. Res. Lett.*, 42, 1352-1359, doi:10.1002/2014GL062700.

Iyemori, T., Takeda, M., Nose, M., Odagi, Y., and Toh, H. (2010). Mid-latitude Geomagnetic Indices ASY and SYM for 2009 (Provisional). In *Internal Report of Data Analysis Center for Geomagnetism and Space Magnetism*, Kyoto University, Japan.

Kataoka, R., et al. (2015). Pileup accident hypothesis of magnetic storm on 17 March 2015. *Geophys. Res. Lett.*, 42, 5155-5161, doi:10.1002/2015GL064816.

Kepko, L., McPherron, R. L., Amm, O., et al. (2015). Substorm Current Wedge Revisited. *Space Sci Rev*, 190, 1-46, doi:10.1007/s11214-014-0124-9.

Liou, K., Sotirelis, T., and Mitchell, E. J. (2018). North-South Asymmetry in the Geographic Location of Auroral Substorms correlated with Ionospheric Effects. *Sci Rep* 8, 17230, doi:10.1038/s41598-018-35091-2.

Liu, Y. D., et al. (2015). Plasma and magnetic field characteristics of solar coronal mass ejections in relation to geomagnetic storm intensity and variability. *Astrophys. J. Lett.*, 809, L34, doi:10.1088/2041-8205/809/2/L34.

Marubashi, K., et al. (2016). The 17 March 2015 storm: the associated magnetic flux rope structure and the storm development. *Earth Planets Space*, 68, 173, doi:10.1186/s40623-016-0551-9.

McPherron, R. I. (1979). Magnetospheric substorms. *Rev. Geophys.*, 17, 657.

Newell, P. T., and Gjerloev, J. W. (2011). Evaluation of SuperMAG auroral electrojet indices as indicators of substorms and auroral power. *J. Geophys. Res.*, 116, A12211, doi:10.1029/2011JA016779.

Newell, P. T., and Gjerloev, J. W. (2012). SuperMAG-Based Partial Ring Current Indices. *J. Geophys. Res.*, 117, doi:10.1029/2012JA017586.

Olsen, N., Hulot, G., Lesur, V., Finlay, C. C., Beggan, C., Chulliat, A., Sabaka, T. J., Floberghagen, R., Friis-Christensen, E., Haagmans, R., Kotsiaros, S., Lhr, H., Tffner-Clausen, L., and Vigneron, P. (2015). The Swarm Initial Field Model for the 2014 geomagnetic field. *Geophys. Res. Lett.*, 42, 1092-1098, doi:10.1002/2014GL062659.

Olsen, N., Stolle, C., Floberghagen, R., Hulot, G., and Kuvshinov, A. (2016). Special issue Swarm science results after 2 years in space. *Earth Planets Space*, 68, 13, doi:10.1186/s40623-016-0546-6.

Pearson, K. (1895). Notes on regression and inheritance in the case of two parents. *P. R. Soc. London*, 58, 240-242.

Papadimitriou, C., Balasis, G., Daglis, I. A., and Giannakis, O. (2018). An initial ULF wave index derived from two years of Swarm observations. *Ann. Geophys.*, 36, 287-299, doi:10.5194/angeo-36-287-2018.

Sugiura, M., and Kamei, T. (1981). IAGA Bulletin N°40, http://wdc.kugi.kyoto-u.ac.jp/dstdir/dst2/onDstindex.html.

Tffner-Clausen, L., Lesur, V., Olsen, N., and Finlay, C. (2016). In-flight scalar calibration and characterisation of the Swarm magnetometry package. *Earth, Planets and Space*, 68(1), 129, doi:10.1186/s40623-016-0501-6.

Wang, Y., et al. (2016). On the propagation of a geoeffective coronal mass ejection during 15–17 March 2015. *J. Geophys. Res.*, 121, 7423-7434, doi:10.1002/2016JA022924.

Weygand, J. M., Zesta, E., and Troshichev, O. (2014), Auroral electrojet indices in the Northern and Southern Hemispheres: A statistical comparison, *J. Geophys. Res. Space Physics*, 119, 4819 4840, doi:10.1002/2013JA019377.

Wu, C. C., et al. (2016). The first super geomagnetic storm of solar cycle 24: The St. Patrick's day event (17 March 2015). *Earth Planets Space*, 68, 151, doi:10.1186/s40623-016-0525-y.

Figure1.

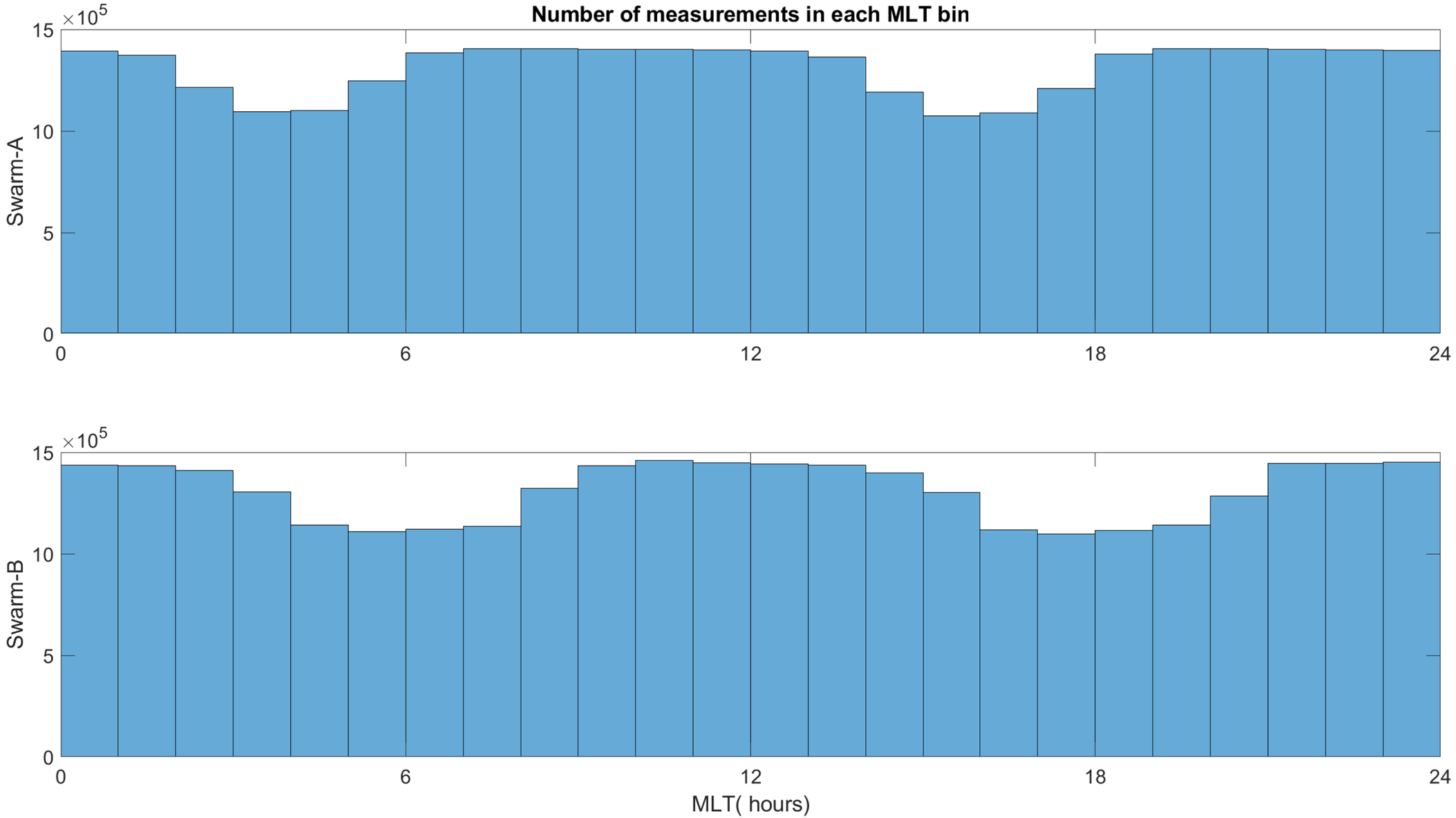
Number of measurements in each MLT bin
×10^5
15
10
5
0
Swarm-A
0
6
12
18
24
×10^5
15
10
5
0
Swarm-B
0
6
12
18
24
MLT(hours)

Figure2.

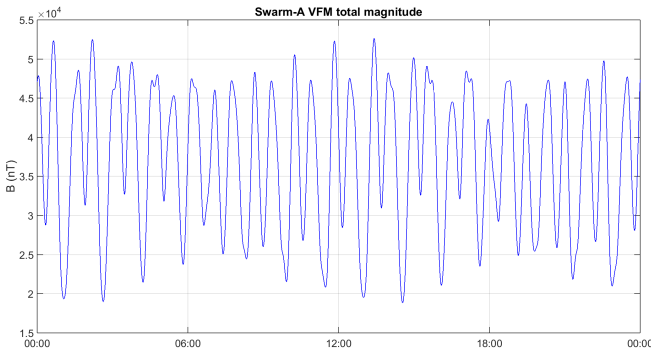

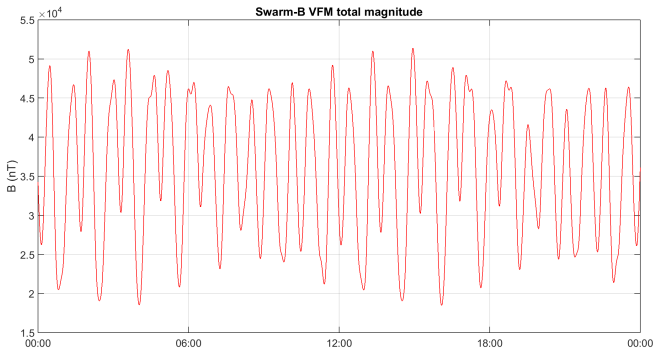

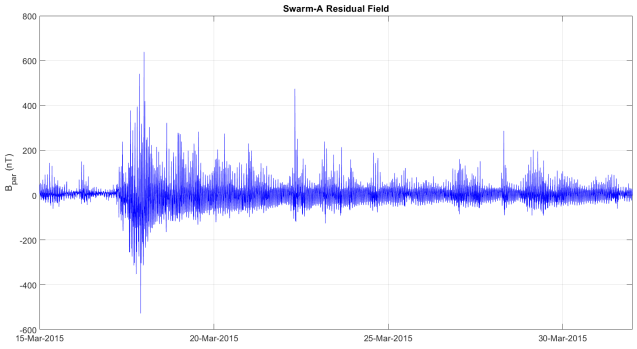

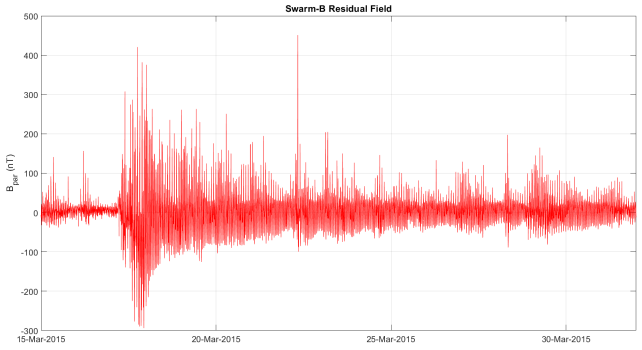

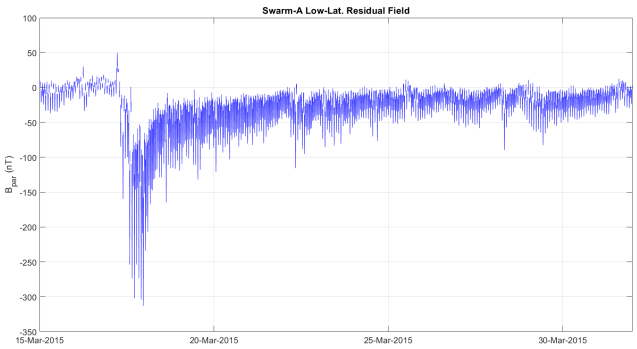

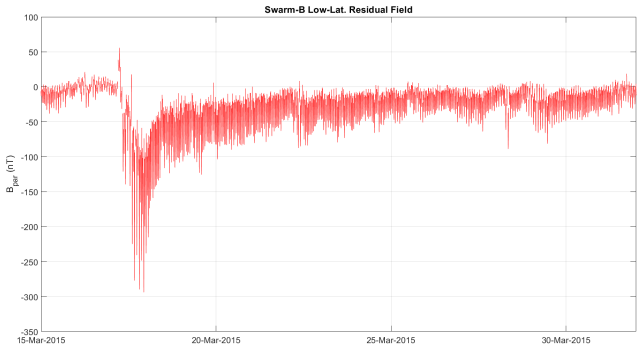

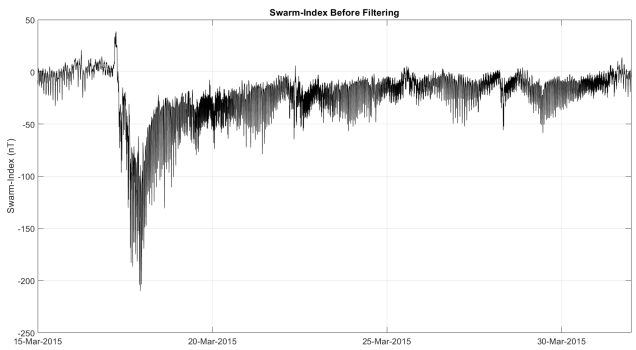

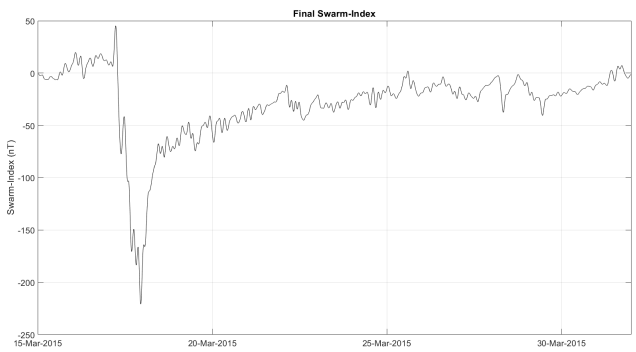

Raw data

Residual
(raw data - CHAOS-6)

Keep only low
latitudes

Combined & interpolated
series

Filtered & transformed
series

Figure3.

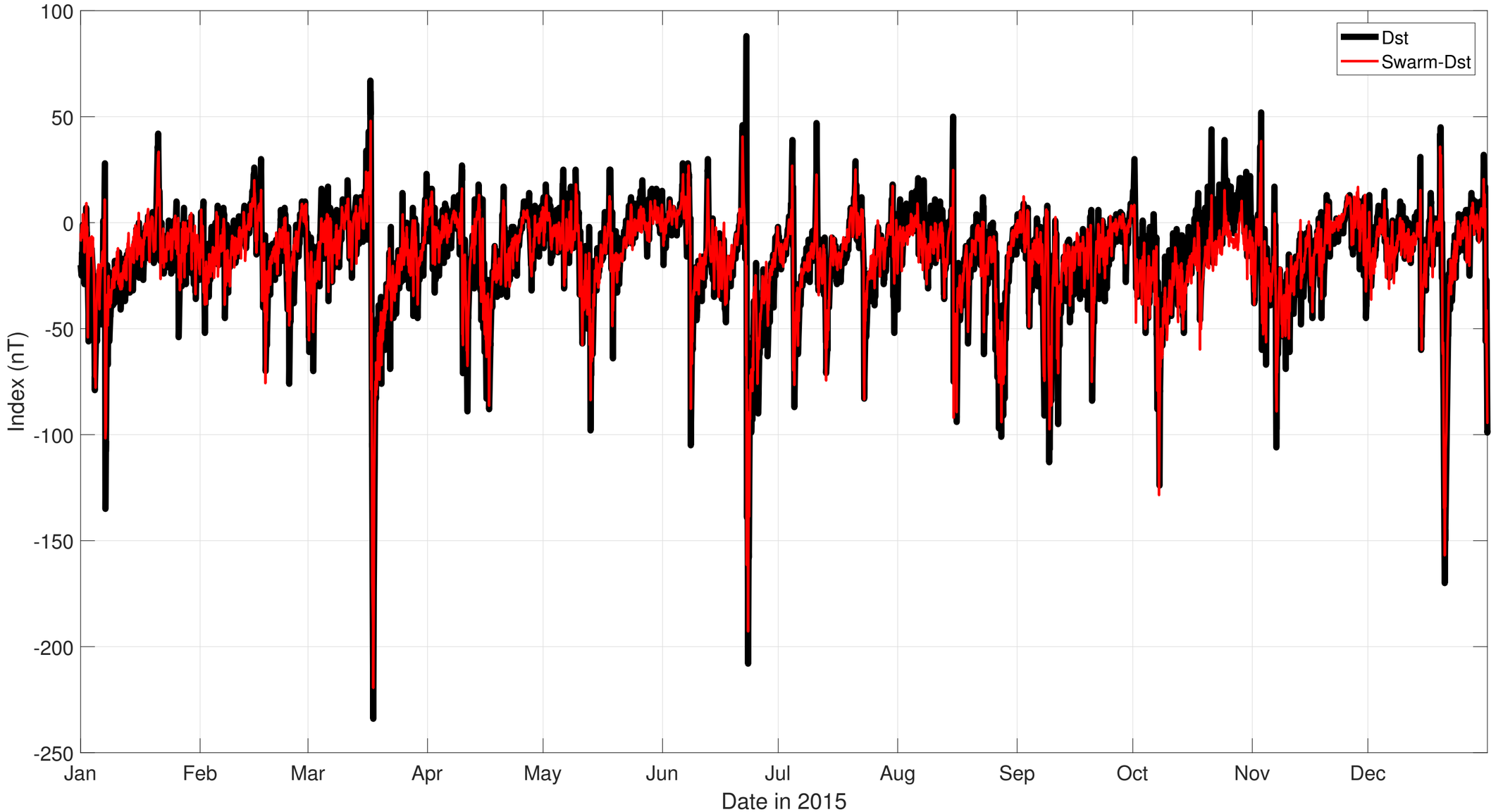
Dst
Swarm-Dst
100
50
0
-50
-100
-150
-200
-250
Index (nT)
Jan
Feb
Mar
Apr
May
Jun
Jul
Aug
Sep
Oct
Nov
Dec
Date in 2015

Figure4.

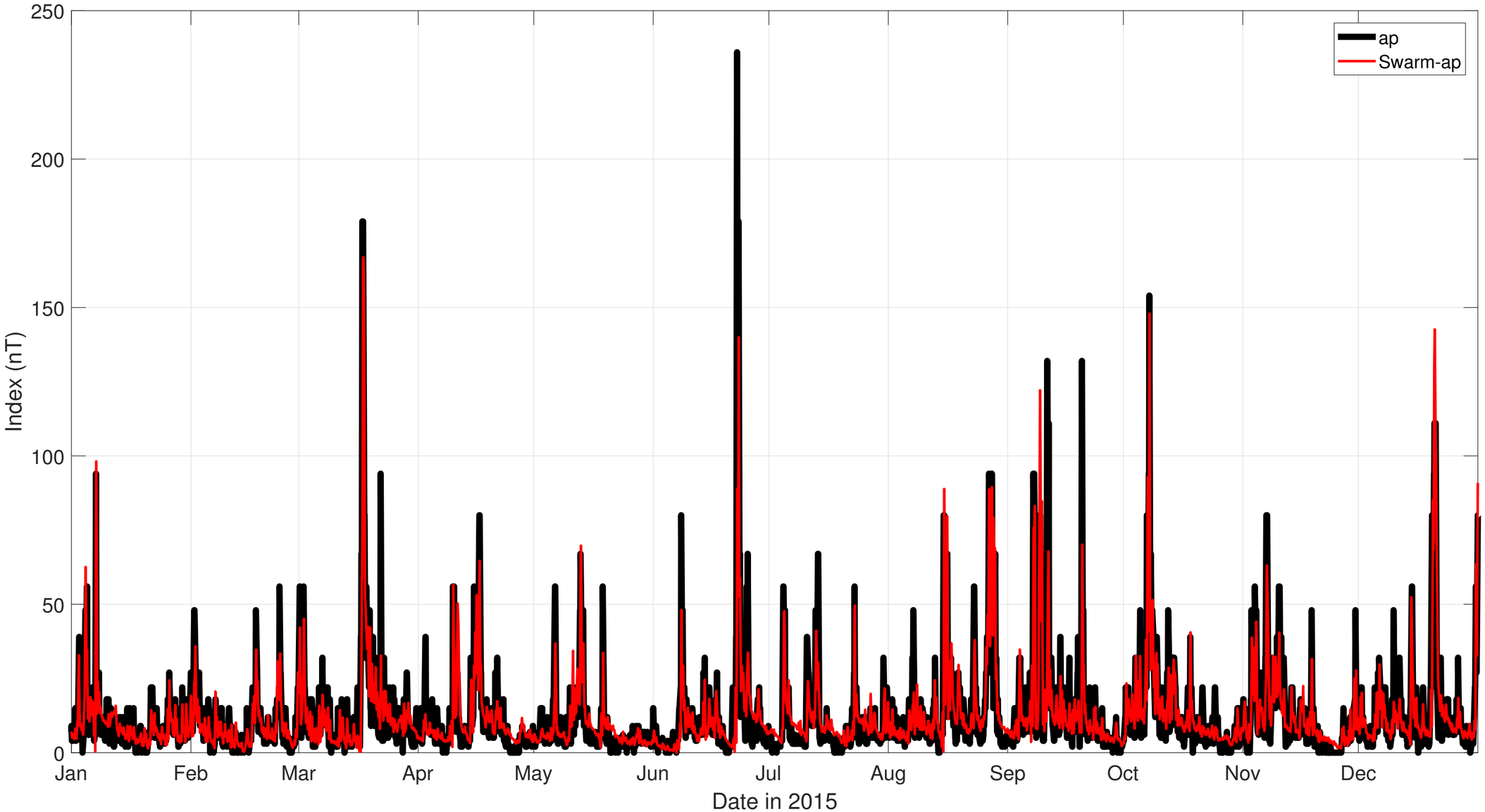
250
200
150
100
50
0
Index (nT)
Jan
Feb
Mar
Apr
May
Jun
Jul
Aug
Sep
Oct
Nov
Dec
Date in 2015
ap
Swarm-ap

Figure5.

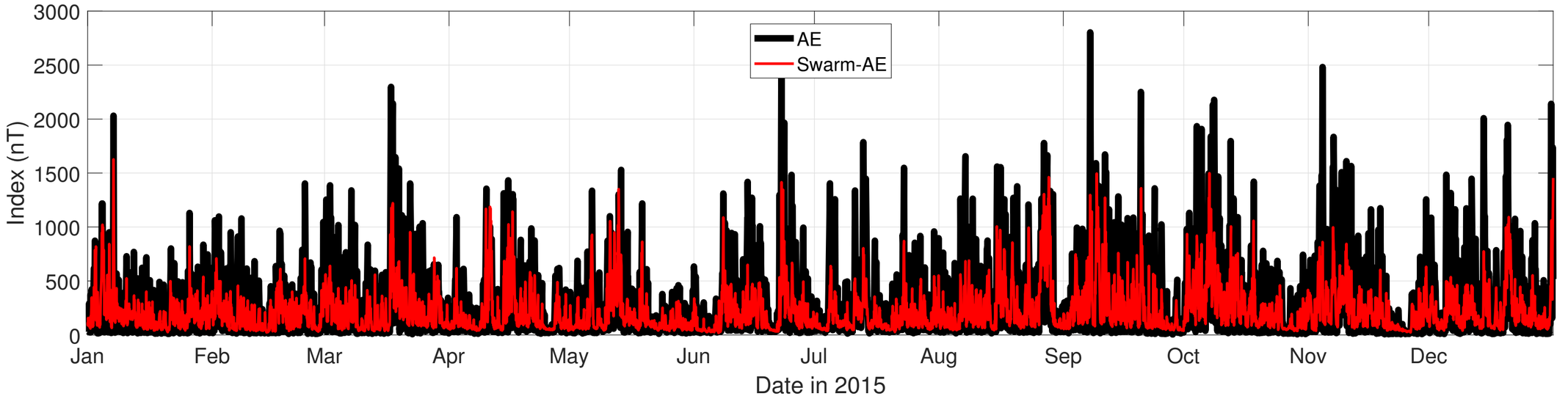
AE
Swarm-AE
Index (nT)
3000
2500
2000
1500
1000
500
0
Jan
Feb
Mar
Apr
May
Jun
Jul
Aug
Sep
Oct
Nov
Dec
Date in 2015

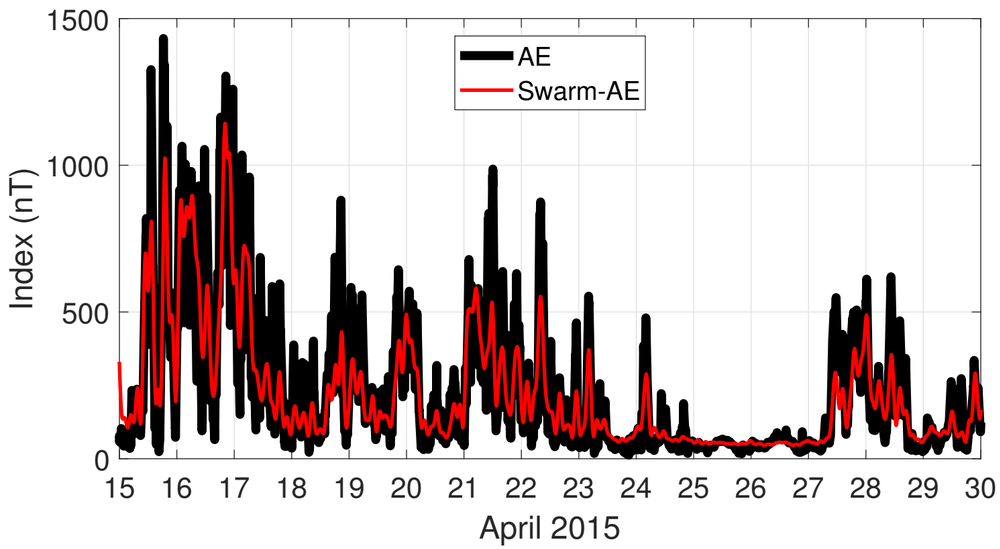
AE
Swarm-AE
Index (nT)
1500
1000
500
0
15 16 17 18 19 20 21 22 23 24 25 26 27 28 29 30
April 2015

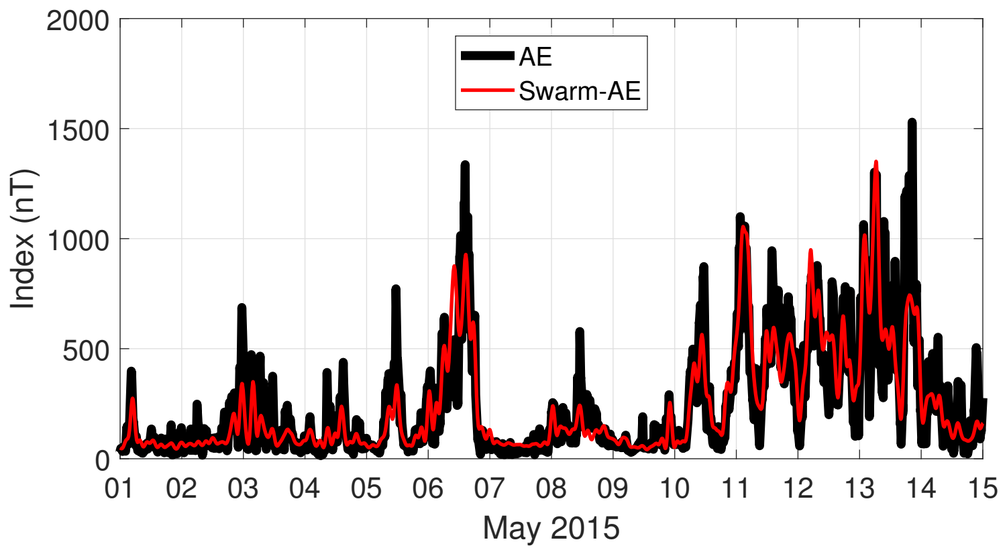
AE
Swarm-AE
Index (nT)
2000
1500
1000
500
0
01 02 03 04 05 06 07 08 09 10 11 12 13 14 15
May 2015

Figure6.

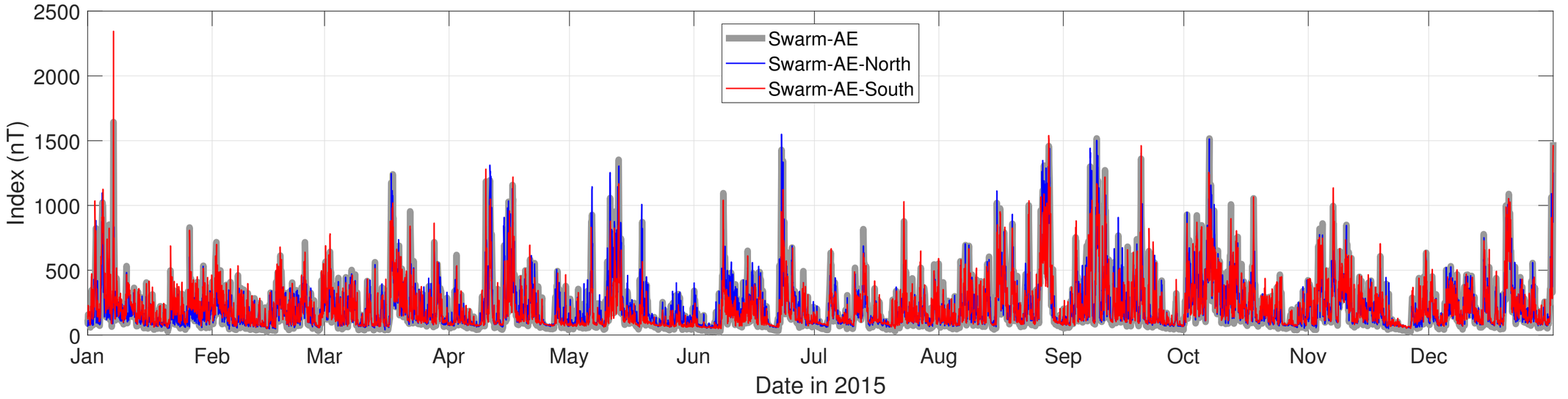
Swarm-AE
Swarm-AE-North
Swarm-AE-South
Index (nT)
2500
2000
1500
1000
500
0
Jan
Feb
Mar
Apr
May
Jun
Jul
Aug
Sep
Oct
Nov
Dec
Date in 2015

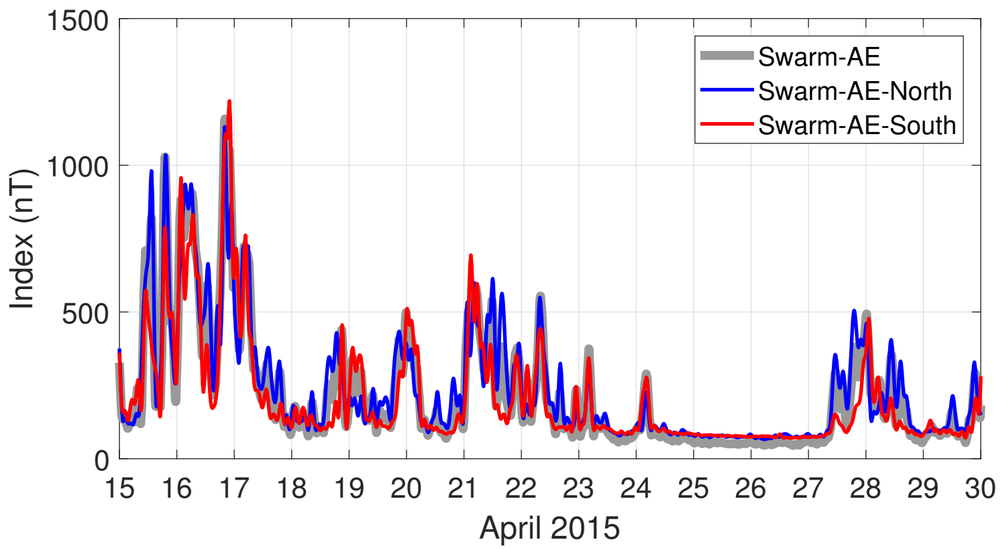
Swarm-AE
Swarm-AE-North
Swarm-AE-South
Index (nT)
1500
1000
500
0
15 16 17 18 19 20 21 22 23 24 25 26 27 28 29 30
April 2015

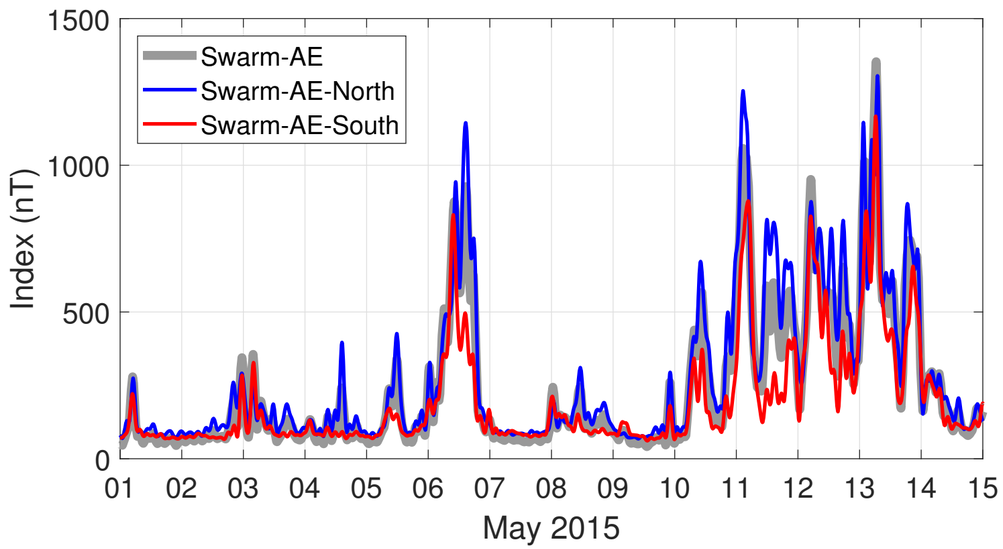
Swarm-AE
Swarm-AE-North
Swarm-AE-South
Index (nT)
1500
1000
500
0
01 02 03 04 05 06 07 08 09 10 11 12 13 14 15
May 2015

Figure7.

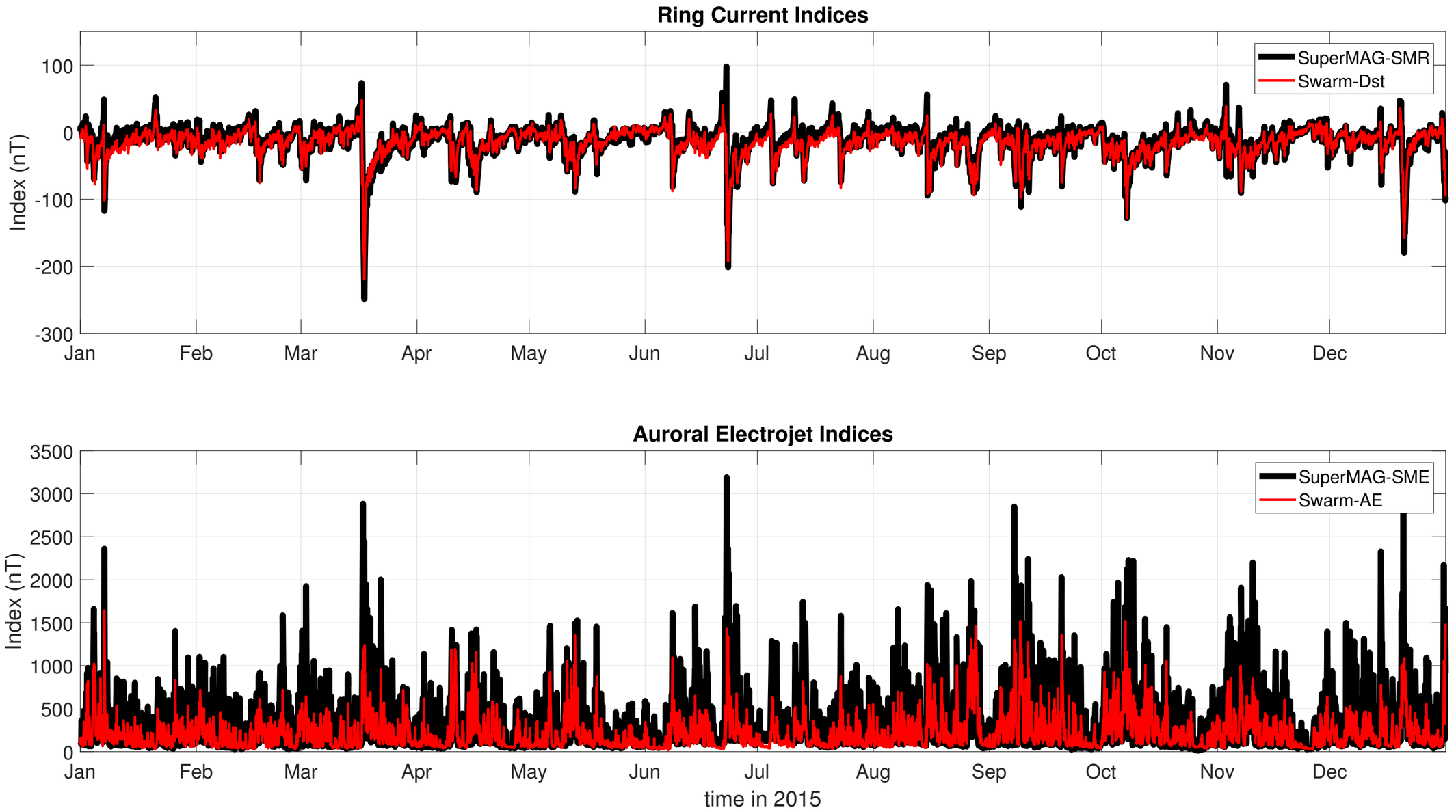
Ring Current Indices
SuperMAG-SMR
Swarm-Dst
Index (nT)
100
0
-100
-200
-300
Jan
Feb
Mar
Apr
May
Jun
Jul
Aug
Sep
Oct
Nov
Dec
Auroral Electrojet Indices
SuperMAG-SME
Swarm-AE
Index (nT)
3500
3000
2500
2000
1500
1000
500
0
time in 2015